

Theoretical Insight on the S → O Photoisomerization of DMSO Complexes of Ru(II)

Daniel A. Lutterman,[†] Aaron A. Rachford,[‡] Jeffrey J. Rack,^{‡,*} and Claudia Turro^{†,*}

Department of Chemistry, The Ohio State University, Columbus, Ohio 43210, and Department of Chemistry and Biochemistry, Nanoscale and Quantum Phenomena Institute, Ohio University, Athens, Ohio 45701

Received: April 2, 2009; Revised Manuscript Received: August 31, 2009

Complexes of the type [Ru(tpy)(L)(dmsO)]ⁿ⁺ (where tpy = 2,2':6',2''-terpyridine; L = 2,2'-bipyridine (bpy), *n* = 2; *N,N,N',N'*-tetramethylethylenediamine (tmen), *n* = 2; acetylacetonate (acac), *n* = 1; oxalate (ox), *n* = 0; malonate (mal), *n* = 0) were investigated by density functional theory (DFT). The results do not support a promoting role for the dσ* ligand field (LF) states during excited state S → O isomerization. Instead, the calculations show that the formation of a Ru(III) center is important in the isomerization, along with the identity of the ancillary bidentate ligand. The present work shows that the orbital contributions from the bidentate ligand to the HOMO, which is typically centered on the ruthenium, plays an important role in the photochemical and oxidative reactivity of the complexes.

Introduction

Ruthenium polypyridyl complexes, such as [Ru(bpy)₃]²⁺ (bpy = 2,2'-bipyridine),¹ have potential applications in various fields, including the conversion of solar energy,^{2,3} sensing and signaling,^{4–8} therapeutic agents,^{9–12} and information storage.^{4,13} In particular, complexes of ruthenium that possess photoisomerizable dmsO (dmsO = dimethyl sulfoxide) ligands may be useful for the latter, since the S → O isomerization can result in marked changes in the absorption and emission maxima of the complexes.¹⁴

The photochemistry and photophysics of ruthenium polypyridine chemistry are dominated by the interaction of the lowest-energy ³MLCT (metal-to-ligand charge-transfer) states with the thermally accessible ligand field (LF) states.^{15–29} Typically, the lowest energy ³MLCT excited state is characterized by a formally oxidized ruthenium +3 atom and a formally reduced polypyridine ligand. The one-electron oxidation potential of the metal and one-electron reduction potential of the ligand provide an estimation of the MLCT energy and the background for the well-known correlation between electrochemical and photochemical parameters observed in these complexes.^{30–33} Thermal population of LF states is the principal mechanism for depopulation of the ³MLCT excited states and subsequent decrease in the lifetime of the excited state.¹⁹ This deactivation is typically undesirable, since much of the motivation of the work in this area is to access the potential energy stored in the ³MLCT state, as this energy may be used to drive other reactions, including those in solar energy conversion.

It was recently reported that certain ruthenium polypyridine dimethyl sulfoxide complexes undergo excited state S → O isomerization following excitation with visible light.^{34–41} The magnitude of the isomerization quantum yields (Φ_{S→O}) are much greater than those typically observed for photosubstitution of bound monodentate ligands by exogenous ligands or solvent.⁴² For example, the photosubstitution quantum yield of acetonitrile by pyridine in [Ru(tpy)(bpy)(CH₃CN)] (tpy = [2,2':6',2'']-terpyridine) in a 1.0 M pyridine solution in acetonitrile is 0.0016. The separate work of Sauvage, McMillin, and Walsh demonstrates that photo-

substitution is a dissociative process involving population of Ru-L dσ* LF states.^{43–45} A convincing observation in these studies is that osmium polypyridine complexes do not readily undergo photosubstitution, presumably due to the inaccessibility of the LF states which lie at higher energies in osmium complexes.

In the complexes described here, the large isomerization quantum yields and the observation of isomerization in osmium dmsO complexes argues against a promoting role for LF states in these systems and supports the notion that isomerization occurs from the CT manifold.^{38,39,41,46} The aim of this computational study is to probe the role of LF states in the photoisomerization of sulfoxide ligands in ruthenium polypyridine complexes as well as to understand the role of the bidentate ligand during isomerization. In particular, attention is paid to identifying those features that explain the observed electro- and photochemical reactivity of these systems. Herein we report our computational results from DFT studies in pursuit of these goals.

Experimental Section

All calculations were performed using the Gaussian03 (G03) program package,⁴⁷ with the Becke three-parameter hybrid exchange and the Lee–Yang–Parr correlation functionals (B3LYP).^{48–50} The 6-31G* basis set was used for H, C, N, O, and S (using five pure d functions),⁵¹ along with the Stuttgart/Dresden (SDD) energy-consistent pseudopotentials for Ru.^{52,53} All geometry optimizations were performed in C₁ symmetry (D₃ for [Ru(bpy)₃]²⁺) with subsequent vibrational frequency analysis to confirm that each stationary point was a minimum on the potential energy surface. Orbital analysis was computed using Molekel 4.3.win32.⁵⁴

The percentage of ruthenium character in some of the occupied (canonical) molecular orbitals (MOs) in the complexes was calculated from a full population analysis, using eq 1

$$\% \text{ Ru character} = \frac{\sum \phi_{\text{Ru}}^2}{\sum \phi_{\text{all}}^2} \times 100\% \quad (1)$$

where Σφ_i² (*i* = Ru or all) is the sum of the squares of the eigenvalues associated with the ruthenium atomic orbital (AO)

* Authors to whom correspondence should be addressed: turro@chemistry.ohio-state.edu and rackj@ohio.edu.

[†] The Ohio State University.

[‡] Ohio University.

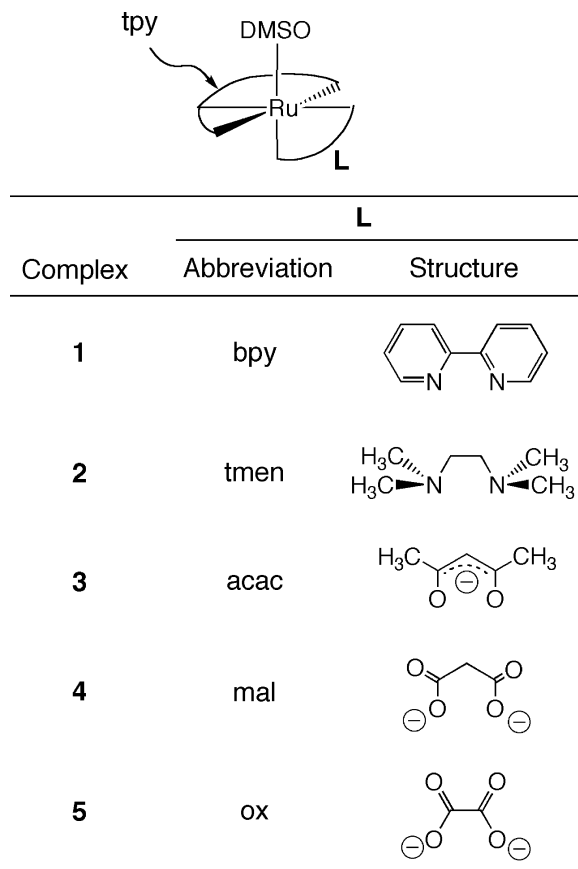


Figure 1. Schematic representation of the molecular structures of $[\text{Ru}(\text{tpy})(\text{L})(\text{dmsO})]^{2+}$ complexes showing the structures of the ligand L with the numbering scheme.

and all of the AOs in a particular MO, respectively. This calculation was performed on the HOMO of each complex and also on each of the three to six highest occupied MOs that had significant metal character, and these values were then averaged. Because the HOMO and the three highest occupied MOs of $[\text{Ru}(\text{bpy})_3]^{2+}$ are widely accepted to be centered on the ruthenium atom (pseudo- t_{2g} set), similar calculations were also performed on this complex for comparison. The vertical singlet transition energies of the complexes were computed at the time-dependent density functional theory (TD-DFT) level within G03 using the ground state optimized structure.

Results and Discussion

Photoisomerization from S-bonded to O-bonded dmsO has been observed in $[\text{Ru}(\text{tpy})(\text{bpy})(\text{dmsO})]^{2+}$ (**1**; tpy = 2,2':6',2''-terpyridine, bpy = 2,2'-bipyridine) and $[\text{Ru}(\text{tpy})(\text{tmen})(\text{dmsO})]^{2+}$ (**2**; tmen = *N,N,N',N'*-tetramethylethylenediamine) complexes, which possess bidentate ligands that are a π -stabilizing and σ -donor only, respectively. The structures of these and related complexes are displayed in Figure 1. In contrast, S → O photoisomerization of the dmsO ligand is not observed in complexes with oxygen π -donor bidentate ligands, such as $[\text{Ru}(\text{tpy})(\text{acac})(\text{dmsO})]^+$ (**3**; acac = acetylacetonate), $[\text{Ru}(\text{tpy})(\text{mal})(\text{dmsO})]$ (**4**; mal = malonate), and $[\text{Ru}(\text{tpy})(\text{ox})(\text{dmsO})]$ (**5**; ox = oxalate), also shown in Figure 1. The S → O photoisomerization quantum yields ($\Phi_{\text{S} \rightarrow \text{O}}$) for **1–5** are listed in Table 1. Notably, **1** and **2** feature $\Phi_{\text{S} \rightarrow \text{O}}$ values that are orders of magnitude greater than those measured for **3–5**.

Shown in Figure 2 are the calculated molecular orbital energy diagrams for **1–5**. The tpy π^* LUMOs are set at the same

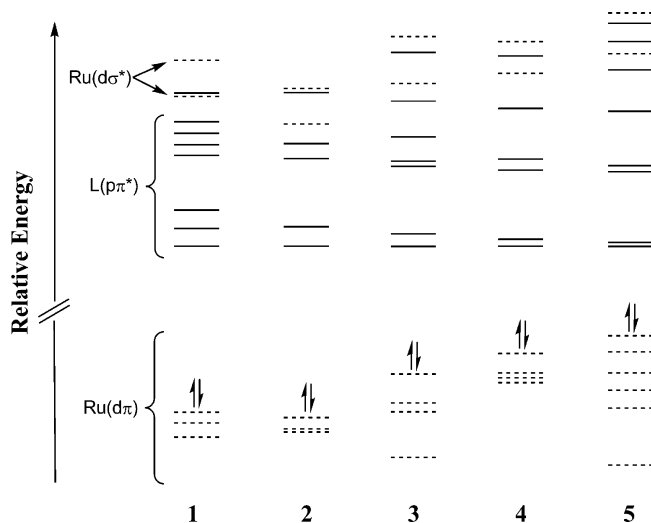


Figure 2. MO diagrams for **1–6**, distinguishing orbitals with metal character (---) from orbitals centered on the ligands (—). The LUMOs were set at the same energy in all complexes.

TABLE 1: Absorption Maxima, Photoisomerization Data, Irreversible Oxidation Potentials, and Percentage of Ruthenium Character in the HOMOs for S-Bound **1–5**

complex	L	$\lambda_{\text{abs}}/\text{nm}^a$	Φ_{iso}^a	$E^{\text{ox}}/a.b$	% Ru ^c	av % Ru ^d
1	bpy	412	0.024	1.67	78.9	76.4
2	tmen	429	0.007	1.65	83.2	80.1
3	acac	468	<0.0001	0.95	56.6	59.4
4	mal	502	0	0.86	57.0	46.9
5	ox	485	0	0.82	23.8	42.5

^a From ref 38. ^b In CH_2Cl_2 or CH_3CN , 0.1 M Bu_4NPF_6 vs Ag/AgCl .

^c Ru contribution in HOMO. ^d Ru contribution to the average of all highest occupied MOs with significant Ru(d) contribution (see text).

energy in the figure in order to provide a reference point for the comparison of the electronic structures of **1–5**. Since the observed reduction potentials ($\text{tpy}^{0/-}$) for these and other ruthenium terpyridine complexes are similar, it is expected that the tpy-localized LUMOs should lie at similar or nearly identical energies. The HOMO–LUMO gap generally decreases in the progression from **1** to **5**, due to the rise of the ruthenium-based HOMO as the π -donor character of the bidentate ligand increases across the series. The decrease in the Ru-based oxidation potential across the series listed in Table 1 is consistent with the calculated changes in the energy of the HOMO for each complex.³⁸ Furthermore, the calculated HOMO–LUMO energy gap agrees well with the red shift of the lowest energy visible MLCT transition also observed from **1** and **2** to **3–5** (Table 1).^{37,38} At significantly higher energy, Figure 2 also shows the ruthenium $d\sigma^*$ orbital set for each compound, which are related to the LF states in each complex. The energies of the $d\sigma^*$ orbital set are largely invariant with the exception of compound **2**, for which these orbitals lie at slightly lower energy. The following is a discussion of the results from calculations of these complexes as it pertains to their photoisomerization quantum yields.

$[\text{Ru}(\text{tpy})(\text{L})(\text{dmsO})]^{2+}$ (L = bpy, tmen). The calculated molecular orbital (MO) diagram for $[\text{Ru}(\text{tpy})(\text{bpy})(\text{dmsO})]^{2+}$ (**1**) shown in Figure 2 is consistent with previous computational results.⁵⁵ A set of three occupied metal-centered MOs is comprised of the highest occupied molecular orbital (HOMO), HOMO-1, and HOMO-2 of **1** (Figure 2); these occupied orbitals will be referred to as the $\text{Ru}(d\pi)$ set. A pictorial representation of the HOMO of **1** is shown in Figure 3a. This MO is

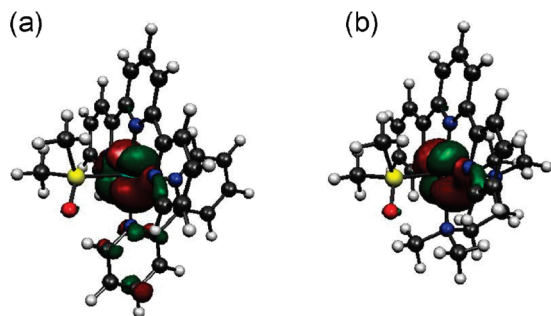


Figure 3. The HOMOs of complexes (a) **1**, (b) **2** and (c) **3** drawn with isovalue = 0.04.

predominantly ruthenium $d\pi$ in character with modest contribution from the terpyridine and bipyridine rings and negligible contribution from the sulfoxide. There is evidence of a π -bonding interaction between the sulfur and ruthenium atoms in the HOMO-1 and HOMO-2 (Supporting Information). It is this interaction that appears to shift the $\text{Ru}^{3+/2+}$ reduction potential to large, positive values and shift the MLCT absorption maximum toward the blue, as compared to $[\text{Ru}(\text{bpy})_3]^{2+}$.³⁹ The antibonding counterpart with orbital contributions mainly from the dmsoligand is denoted as LUMO+13 – LUMO+16 (Supporting Information). Eight $L(\pi^*)$ MOs of **1** are centered on the tpy and bpy ligands, seven of which comprise the lowest unoccupied MOs. Two metal-centered unoccupied orbitals, $\text{Ru}(d\sigma^*)$, are found at higher energy than the $\text{tpy}(\pi^*)$ MOs (Figure 2), consistent with expectation. The energy difference between the highest energy $\text{Ru}(d\pi)$ and the lowest energy $\text{Ru}(d\sigma^*)$ orbital, Δ_o , for **1** was found to be 5.45 eV (43957 cm^{-1}), which is in accord with related $\text{Ru}(\text{II})$ complexes.^{56,58} The MO diagram of **2** exhibits a similar orbital arrangement to that of **1** (Figure 2). The HOMO of **2** contains orbital contributions mostly from the ruthenium atom (Figure 3b), with a modest contribution from the terpyridine and negligible contributions from the tmen and dmsoligands. Since tmen is a σ -donor ligand and bpy is a π -acceptor ligand, Δ_o is smaller in **2** by 0.30 eV (2662 cm^{-1}) as compared to **1**.

On the basis of the computational results of **1** and **2**, the $\text{S} \rightarrow \text{O}$ photoisomerization does not stem from a low-lying ^3LF dd state(s) in these complexes. If this were the case, one would expect a larger photoisomerization quantum yield for **2** than for **1**. Results from TD-DFT calculations confirm that the lowest energy spin-allowed transitions for **1** and **2** are $\text{Ru}(d\pi) \rightarrow \text{tpy}(\pi^*)$ metal-to-ligand charge transfer ($^1\text{MLCT}$) in character (Tables S1 and S2 in Supporting Information).^{38,55} It should be noted that in **1** the lowest excited state with any ^1LF dd character is ES_{10} which lies 0.4 eV lower at 3.54 eV above the ground state, while in **2** the lowest energy excited state with such character lies 3.14 eV (ES_5) above the ground state. It can be

assumed that this stabilization in the ^1LF dd state of **2** compared to **1** is mirrored in the triplet manifold and provides an explanation for why the photoisomerization quantum yield is reduced in **2**. Presumably, the lowest energy ^3LF dd state diminishes the $^3\text{MLCT}$ lifetime inhibiting isomerization. From the comparison of the reactivity of **1** and **2**, it appears that the most important factor for isomerization is formal oxidation of the ruthenium center, either by electrochemical oxidation or through photogeneration of the $^3\text{MLCT}$. The electrochemical oxidation of both complexes, **1** and **2**, shows evidence of isomerization further supporting the idea that a $\text{Ru}(\text{III})$ is necessary for the isomerization of the dmsoligand.³⁸

[Ru(tpy)(acac)(dmsol)]⁺ and **[Ru(tpy)(L)(dmsol)]** (**L** = mal, ox). While **3** exhibits a very small isomerization quantum yield, neither **4** nor **5** feature photochemical or electrochemical $\text{S} \rightarrow \text{O}$ isomerization. DFT calculations were performed to elucidate the electronic structure of these complexes, as well as to identify a theoretical explanation for the differences in electrochemical and photochemical isomerization among the complexes. Accordingly, the MO diagrams of **3–5** are shown in Figure 2. The calculations show a decrease in Δ_o for **3–5** relative to **1** and **2**, which can be attributed to the π -donor nature of the acac, mal, and ox ligands, respectively. For complexes **3–5**, Δ_o was found to be 5.11 eV (41215 cm^{-1}), 4.98 eV (40166 cm^{-1}), and 5.01 eV (40408 cm^{-1}), respectively.

The highest occupied MOs of **3–5** show significant orbital contribution from both $\text{Ru}(d\pi)$ orbitals and ligand $p\pi$ orbitals. The acac, mal, and ox ligand $p\pi$ orbitals in **3**, **4**, and **5**, respectively, interact with the pseudo- t_{2g} $\text{Ru}(d\pi)$ set of metal-centered orbitals producing new linear combinations of orbitals with significant ligand contribution. The HOMOs of **3–5** are shown in Figure 4 and can be compared to those of **1** and **2** (Figure 3). The difference in metal contribution to the character of the HOMOs of **3–5** relative to those of **1** and **2** is evident from a visual comparison of Figures 3 and 4. For complexes **1** and **2**, the HOMOs possess 78.9% and 83.2% ruthenium character, respectively (Table 1), which match well with the 80.8% character calculated for the HOMO of $[\text{Ru}(\text{bpy})_3]^{2+}$ (Supporting Information). In contrast, the HOMOs of complexes **3–5** have significant ligand contribution resulting in 56.6%, 57.0%, and 23.8% ruthenium character, respectively. The mixing of the $\text{Ru}(d\pi)$ MOs with filled ligand orbitals disperses the ruthenium character over more than three orbitals but accordingly decreases the amount of ruthenium character for each individual orbital. For example, complexes **3** and **4** have four $\text{Ru}(d\pi)$ MOs each with significant metal character (Figure 2, dashed lines). The mixing is more pronounced in **5**, for which six occupied MOs exhibit significant metal character. Of these six $\text{Ru}(d\pi)$ MOs in **5**, four have less than 28% ruthenium character (Supporting Information). Averages of the percent

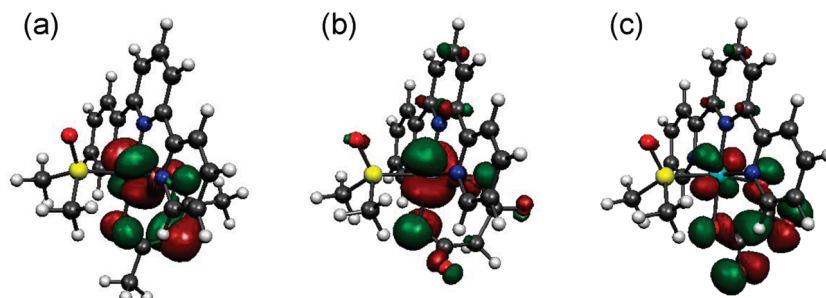


Figure 4. The HOMOs of complexes (a) **4**, (b) **5**, and (c) **6** drawn with isovalue = 0.04.

contribution of ruthenium to the Ru($d\pi$) occupied MOs for **1–5** are also listed in Table 1.

Although the lowest energy excited state of **3–5** is Ru($d\pi$) → $\text{tpy}(\pi^*)$ $^3\text{MLCT}$ in character, in contrast to **1** and **2**, it appears that population of the $^3\text{MLCT}$ excited state in these complexes does not lead to isomerization. If it is assumed that a Ru(III) center is required for isomerization, then the delocalization of charge density among the metal and ligand may hinder isomerization in these complexes. Since the Ru($d\pi$) MOs in **3–5** have less ruthenium character than those of **1**, when oxidized either electrochemically or through excitation into a $^3\text{MLCT}$ state, the formal charge on the ruthenium atom is less than +3. In terms of reactivity, this reduced charge renders the ruthenium center less susceptible to attack from the nucleophilic sulfoxide oxygen. These calculations reveal that the increased ligand $p\pi$ orbital contribution to the HOMO orbitals in complexes **3–5** reduces or eliminates the electrochemical isomerization. In addition, it may also be inferred that the diminished Δ_0 inhibits photoisomerization through reduction of the $^3\text{MLCT}$ excited state lifetime.

Conclusions

Consistent with experimental results, the calculations demonstrate that the LF states do not promote photoisomerization in these complexes, in contrast to typical photosubstitution or photosolvation mechanisms. The generation of a Ru(III) center, either electrochemically or photochemically through MLCT excitation, is critical for S → O dmsol isomerization to take place in these complexes. The reduction of Ru contribution to the HOMO from >79% in **1** and **2** to ≤57% in **3–5** provides enough electron density from the oxygen π -donor ligands to hinder or eliminate S → O dmsol isomerization in the latter. These results serve as our first attempts to identify the critical orbital interactions present in these excited state isomerizations. Future work will attempt to calculate the dynamic motions operative during isomerization of sulfoxides in dmsol and in chelating sulfoxides.

Acknowledgment. C.T. thanks the National Science Foundation (CHE 0503666) and the Ohio Supercomputer Center for their generous support. J.J.R. thanks Ohio University, NSF (CHE 0809669), and PRF (38071-G3) for partial support of this work. A.A.R. thanks the OU Graduate Student Council for an SEA Award. D.A.L. thanks The Ohio State University for a Presidential Fellowship.

Supporting Information Available: All Cartesian coordinates, TD-DFT results, MOs that shown Ru–S π -bonding, % Ru character of Ru($d\pi$) orbitals, and full population analysis of selected MOs. This material is available free of charge via the Internet at <http://pubs.acs.org>.

References and Notes

- (1) Meyer, T. J. *J. Am. Chem. Soc.* **1989**, *111*, 163.
- (2) Lewis, N. S.; Nocera, D. G. *Proc. Natl. Acad. Sci. U.S.A.* **2006**, *103*, 15729.
- (3) Balzani, V.; Campagna, S.; Denti, G.; Juris, A.; Serroni, S.; Venturi, M. *Acc. Chem. Res.* **1998**, *31*, 26.
- (4) de Silva, A. P.; Gunaratne, H. Q. N.; Gunnlaugsson, T.; Huxley, A. J. M.; McCoy, C. P.; Rademacher, J. T.; Rice, T. E. *Chem. Rev.* **1997**, *97*, 1515.
- (5) Turro, N. J.; Barton, J. K. *J. Biol. Inorg. Chem.* **1998**, *3*, 201.
- (6) Martinez-Manez, R.; Sancenon, F. *Chem. Rev.* **2003**, *103*, 4419.
- (7) (a) Drummond, T. G.; Hill, M. G.; Barton, J. K. *Nat. Biotechnol.* **2003**, *21*, 1192. (b) Boon, E. M.; Ceres, D. M.; Drummond, T. G.; Hill, M. G.; Barton, J. K. *Nat. Biotechnol.* **2000**, *18*, 1096.
- (8) (a) Lutterman, D. A.; Chouai, A.; Sun, Y.; Stewart, C. D.; Dunbar, K. R.; Turro, C. *J. Am. Chem. Soc.* **2008**, *130*, 1163–1170. (b) Sun, Y.; Lutterman, D. A.; Turro, C. *Inorg. Chem.* **2008**, *47*, 6427–6434. (c) Liu, Y.; Chouai, A.; Degtyareva, N. N.; Dunbar, K. R.; Turro, C. *J. Am. Chem. Soc.* **2005**, *127*, 10796–10797.
- (9) (a) Liu, Y.; Turner, D. B.; Singh, T. N.; Chouai, A.; Dunbar, K. R.; Turro, C. *J. Am. Chem. Soc.* **2009**, *131*, 26–27. (b) Liu, Y.; Hammett, R.; Lutterman, D. A.; Joyce, L. E.; Thummel, R. P.; Turro, C. *Inorg. Chem.* **2009**, *48*, 375–385. (c) Liu, Y.; Hammett, R.; Lutterman, D. A.; Thummel, R. P.; Turro, C. *Inorg. Chem.* **2007**, *46*, 6011–6021. (d) Singh, T. N.; Turro, C. *Inorg. Chem.* **2004**, *43*, 7260.
- (10) Clarke, M. *Coord. Chem. Rev.* **2002**, *232*, 69–93.
- (11) Erkkila, K. E.; Odom, D. T.; Barton, J. K. *Chem. Rev.* **1999**, *99*, 2777.
- (12) Rose, M. J.; Mascharak, P. K. *Coord. Chem. Rev.* **2008**, *252*, 2093–2114.
- (13) de Silva, A. P. M.; Nathan, D. *Chem.—Eur. J.* **2004**, *10*, 574.
- (14) (a) Rack, J. J. *Kristallogr.* **2008**, *223*, 356–362. (b) Rack, J. J. *Coord. Chem. Rev.* **2009**, *253*, 78–85.
- (15) Kober, E. M.; Meyer, T. J. *Inorg. Chem.* **1982**, *21*, 3967–3977.
- (16) Caspar, J. V.; Meyer, T. J. *J. Am. Chem. Soc.* **1983**, *105*, 5583–5590.
- (17) Caspar, J. V.; Meyer, T. J. *Inorg. Chem.* **1983**, *22*, 2444–2453.
- (18) Kober, E. M.; Meyer, T. J. *Inorg. Chem.* **1984**, *23*, 3877–3886.
- (19) Juris, A.; Balzani, V.; Barigelletti, F.; Campagna, S.; Belser, P.; Von Zelewsky, A. *Coord. Chem. Rev.* **1988**, *84*, 88–277.
- (20) Lumpkin, R. S.; Kober, E. M.; Worl, L. A.; Murtaza, Z.; Meyer, T. J. *J. Phys. Chem.* **1990**, *94*, 239–243.
- (21) Barigelletti, F.; Flamigni, L.; Balzani, V.; Collin, J.-P.; Sauvage, J.-P.; Sour, A.; Constable, E. C.; Thompson, A. M. W. C. *Coord. Chem. Rev.* **1994**, *132*, 209–214.
- (22) Damrauer, N. H.; Cerullo, G.; Yeh, A.; Boussie, T. R.; Shank, C. V.; McCusker, J. K. *Science* **1997**, *275*, 54–87.
- (23) Baba, A. I.; Shaw, J. R.; Simon, J. A.; Thummel, R. P.; Schmehl, R. H. *Coord. Chem. Rev.* **1998**, *171*, 43–59.
- (24) Damrauer, N. H.; McCusker, J. K. *J. Phys. Chem. A* **1999**, *103*, 8440–8446.
- (25) McCusker, J. K. *Acc. Chem. Res.* **2003**, *36*, 876–887.
- (26) Wang, X.-Y.; Guerso, A. D.; Schmehl, R. H. *J. Photochem. Photobiol., C* **2004**, *5*, 55–77.
- (27) Baranoff, E.; Collin, J.-P.; Flamigni, L.; Sauvage, J.-P. *Chem. Soc. Rev.* **2004**, *33*, 147–155.
- (28) Baitalik, S.; Wang, X.-Y.; Schmehl, R. H. *J. Am. Chem. Soc.* **2004**, *126*, 16304–16305.
- (29) Abrahamsson, M.; Jager, M.; Osterman, T.; Eriksson, L.; Persson, P.; Becker, H.-C.; Johansson, O.; Hammarstrom, L. *J. Am. Chem. Soc.* **2006**, *128*, 12616–12617.
- (30) Lever, A. B. P.; Dodsworth, E. S. *Electrochemistry, Charge Transfer Spectroscopy, and Electronic Structure. In Inorganic Electronic Structure and Spectroscopy, volume II: applications and case studies*; Solomon, E. I., Lever, A. B. P., Eds.; John Wiley & Sons: New York, 1999; pp 227–289.
- (31) Endicott, J. F. *The Photophysics and Photochemistry of Coordination Compounds. In Inorganic Electronic Structure and Spectroscopy, volume II: applications and case studies*; Solomon, E. I., Lever, A. B. P., Eds.; John Wiley & Sons: New York, 1999; pp 291–341.
- (32) Endicott, J. F.; Uddin, M. J. *Coord. Chem. Rev.* **2001**, *219*–221, 687–712.
- (33) Seneviratne, D. S.; Uddin, M. J.; Swayambunathan, V.; Schlegel, H. B.; Endicott, J. F. *Inorg. Chem.* **2002**, *41*, 1502–1517.
- (34) Smith, M. K.; Gibson, J. A.; Young, C. G.; Broomhead, J. A.; Junk, P. C.; Keene, F. R. *Eur. J. Inorg. Chem.* **2000**, 1365–1370.
- (35) Rack, J. J.; Winkler, J. R.; Gray, H. B. *J. Am. Chem. Soc.* **2001**, *123*, 2432–2433.
- (36) Rack, J. J.; Mockus, N. V. *Inorg. Chem.* **2003**, *42*, 5792–5794.
- (37) Rack, J. J.; Rachford, A. A.; Shelker, A. M. *Inorg. Chem.* **2003**, *42*, 7357–7359.
- (38) Rachford, A. A.; Petersen, J. L.; Rack, J. J. *Inorg. Chem.* **2005**, *44*, 8065–8075.
- (39) Rachford, A. A.; Petersen, J. L.; Rack, J. J. *Inorg. Chem.* **2006**, *45*, 5953–5960.
- (40) Rachford, A. A.; Rack, J. J. *J. Am. Chem. Soc.* **2006**, *128*, 14318–14324.
- (41) Butcher, D. P., Jr.; Rachford, A. A.; Petersen, J. L.; Rack, J. J. *Inorg. Chem.* **2006**, *45*, 9178–9180.
- (42) Bonnet, S.; Collin, J.-P.; Sauvage, J.-P. *Inorg. Chem.* **2006**, *45*, 4024–4034.
- (43) Kirchhoff, J. R.; McMillin, D. R.; Marnot, P. A.; Sauvage, J.-P. *J. Am. Chem. Soc.* **1985**, *107*, 1138–1141.
- (44) Suen, H.-F.; Wilson, S. W.; Pomerantz, M.; Walsh, J. L. *Inorg. Chem.* **1989**, *28*, 786–791.
- (45) Hecker, C. R.; Fanwick, P. E.; McMillin, D. R. *Inorg. Chem.* **1991**, *30*, 659–666.

- (46) Mockus, N. V.; Petersen, J. L.; Rack, J. J. *Inorg. Chem.* **2006**, *45*, 8–10.
- (47) Frisch, M. J.; Trucks, G. W.; Schlegel, H. B.; Scuseria, G. E.; Robb, M. A.; Cheeseman, J. R.; Montgomery, J. A., Jr.; Vreven, T.; Kudin, K. N.; Burant, J. C.; Millam, J. M.; Iyengar, S. S.; Tomasi, J.; Barone, V.; Mennucci, B.; Cossi, M.; Scalmani, G.; Rega, N.; Petersson, G. A.; Nakatsuji, H.; Hada, M.; Ehara, M.; Toyota, K.; Fukuda, R.; Hasegawa, J.; Ishida, M.; Nakajima, T.; Honda, Y.; Kitao, O.; Nakai, H.; Klene, M.; Li, X.; Knox, J. E.; Hratchian, H. P.; Cross, J. B.; Adamo, C.; Jaramillo, J.; Gomperts, R.; Stratmann, R. E.; Yazyev, O.; Austin, A. J.; Cammi, R.; Pomelli, C.; Ochterski, J. W.; Ayala, P. Y.; Morokuma, K.; Voth, G. A.; Salvador, P.; Dannenberg, J. J.; Zakrzewski, V. G.; Dapprich, S.; Daniels, A. D.; Strain, M. C.; Farkas, O.; Malick, D. K.; Rabuck, A. D.; Raghavachari, K.; Foresman, J. B.; Ortiz, J. V.; Cui, Q.; Baboul, A. G.; Clifford, S.; Cioslowski, J.; Stefanov, B. B.; Liu, G.; Liashenko, A.; Piskorz, P.; Komaromi, I.; Martin, R. L.; Fox, D. J.; Keith, T.; Al-Laham, M. A.; Peng, C. Y.; Nanayakkara, A.; Challacombe, M.; Gill, P. M. W.; Johnson, B.; Chen, W.; Wong, M. W.; Gonzalez, C.; Pople, J. A. *Gaussian 03, revision C.02*; Gaussian, Inc.: Wallingford, CT, 2004.
- (48) Becke, A. D. *J. Chem. Phys.* **1993**, *98*, 5648.
- (49) Becke, A. D. *Phys. Rev. A: Gen. Phys.* **1988**, *38*, 3098.
- (50) Lee, C.; Yang, W.; Parr, R. G. *Phys. Rev. B: Condens. Matter Mater. Phys.* **1988**, *37*, 785.
- (51) Hehre, W. J.; Radom, L.; Schleyer, P. v. R.; Pople, J. A. *Ab Initio Molecular Orbital Theory*; John Wiley & Sons: New York, 1986.
- (52) Dolg, M.; Stoll, H.; Preuss, H. *Theor. Chim. Acta* **1993**, *85*, 441.
- (53) Wedig, U.; Dolg, M.; Stoll, H. *Quantum Chemistry: The Challenge of Transition Metals and Coordination Chemistry*; NATO ASI series, series C, mathematical and physical sciences, no. 176; D. Reidel Publishing Co.: Dordrecht, The Netherlands, 1986.
- (54) Flükiger, P.; Lüthi, H. P.; Portmann, S.; Weber, J. *MOLEKEL 4.3*; Swiss Center for Scientific Computing: Manno, Switzerland, 2000; www.cscs.ch/molkel.
- (55) Ciofini, I.; Daul, C. A.; Adamo, C. *J. Phys. Chem. A* **2003**, *107*, 11182.
- (56) Olabe, J. A.; Zerga, H. O.; Gentil, L. A. *J. Chem. Soc., Dalton Trans.* **1987**, 1267.
- (57) Toma, H. E.; Giesbrecht, E.; Malin, J. M.; Fluck, E. *Inorg. Chim. Acta* **1975**, *14*, 401.
- (58) Lever, A. B. P. *Inorganic Electronic Spectroscopy*, 2nd ed.; Elsevier: Amsterdam, 1984.

JP903048N